

## Accelerated Publications

---

### Snapshots along an Enzymatic Reaction Coordinate: Analysis of a Retaining $\beta$ -Glycoside Hydrolase<sup>†,‡</sup>

Gideon J. Davies,<sup>\*,§</sup> Lloyd Mackenzie,<sup>||</sup> Annabelle Varrot,<sup>§</sup> Mirosława Dauter,<sup>§</sup> A. Marek Brzozowski,<sup>§</sup> Martin Schülein,<sup>⊥</sup> and Stephen G. Withers<sup>||</sup>

Department of Chemistry, University of York, Heslington, York YO1 5DD, U.K., Department of Chemistry, University of British Columbia, Vancouver V6T 1Z1, Canada, and Novo Nordisk A/S, Novo Allé, DK-2880, Bagsværd, Denmark

Received June 3, 1998; Revised Manuscript Received June 30, 1998

**ABSTRACT:** The enzymatic hydrolysis of *O*-glycosidic linkages is one of the most diverse and widespread reactions in nature and involves a classic "textbook" enzyme mechanism. A multidisciplinary analysis of a  $\beta$ -glycoside hydrolase, the Cel5A from *Bacillus agaradhaerens*, is presented in which the structures of each of the native, substrate, covalent-intermediate, and product complexes have been determined and their interconversions analyzed kinetically, providing unprecedented insights into the mechanism of this enzyme class. Substrate is bound in a distorted <sup>1</sup>S<sub>3</sub> skew-boat conformation, thereby presenting the anomeric carbon appropriately for nucleophilic attack as well as satisfying the stereoelectronic requirements for an incipient oxocarbenium ion. Leaving group departure results in the trapping of a covalent  $\alpha$ -glycosyl-enzyme intermediate in which the sugar adopts an undistorted <sup>4</sup>C<sub>1</sub> conformation. Finally, hydrolysis of this intermediate yields a product complex in which the sugar is bound in a partially disordered mode, consistent with unfavorable interactions and low product affinity.

Glycoside hydrolases are a ubiquitous group of proteins and have been widely studied since the seminal structure determination of hen egg white lysozyme (HEWL) in the 1960s (1, 2). The massive chemical and structural diversity of naturally occurring glycosides is matched by an equally

impressive array of hydrolytic enzymes: over 60 sequence-distinct families of these enzymes are now known (3, 4). Their functions range from the simple hydrolysis of stored glycosides to viral invasion processes and the control and mediation of cell–cell interactions (for review see ref 5). The catalytic mechanisms of these enzymes have attracted much interest not least because of their prevalence in textbooks, the widespread occurrence of genetically inherited disorders of glycoside hydrolysis, and the potential for inhibitors of these enzymes to act as new therapeutic agents for the treatment of viral diseases: glycosidase and glycoprotein processing inhibitors offer potential for the treatment of viral infections such as those caused by HIV and influenza (6, 7).

Hydrolysis of the glycosidic bond can occur with either inversion or net retention of the anomeric configuration, and

---

<sup>†</sup> This work was funded, in part, by the Biotechnology and Biological Sciences Research Council, Novo Nordisk A/S, the European Union (Contract BIO4-CT97-2303), The Protein Engineering Centre of Excellence of Canada, and the Universities of York and British Columbia. G.J.D. is a Royal Society University Research Fellow.

<sup>‡</sup> Coordinates for the structures described in this paper have been deposited with the Brookhaven Protein Data Bank (Accession numbers 3A3H, 4A3H, 5A3H, 6A3H, and 7A3H).

<sup>\*</sup> To whom correspondence should be addressed. Tel: 44-1904-432596. Fax: 44-1904-410519. E-mail: davies@york.york.ac.uk.

<sup>§</sup> University of York.

<sup>||</sup> University of British Columbia.

<sup>⊥</sup> Novo Nordisk A/S.

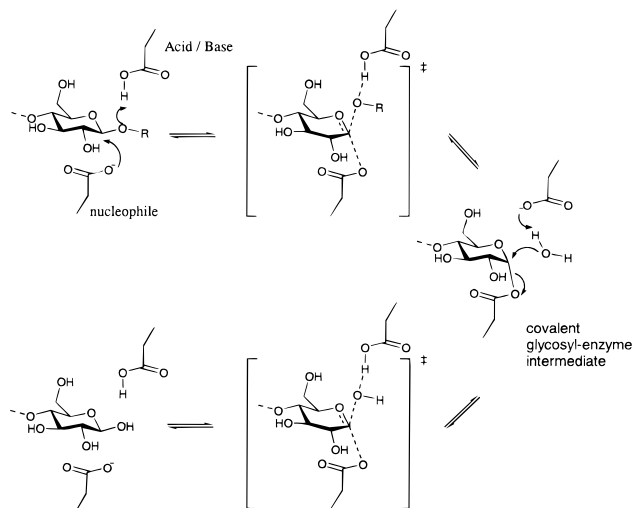


FIGURE 1: Double-displacement reaction for retaining  $\beta$ -glycoside hydrolases: a covalent glycosyl-enzyme intermediate is formed and subsequently hydrolyzed via oxocarbenium ion transition states.

enzymes within a family follow the same stereochemical course (5, 8). Catalysis by the vast majority of the retaining glycosyl hydrolases involves the general acid/base catalyzed formation and subsequent hydrolysis of a covalent glycosyl-enzyme intermediate via transition states which possess substantial oxocarbenium ion character (Figure 1), essentially as outlined by Koshland in 1953 (9). Support for this mechanism has been obtained in a number of ways (reviewed in refs 10 and 11). Of particular importance has been the measurement of  $\alpha$ -secondary deuterium kinetic isotope effects of  $k_H/k_D > 1$  for both steps. Such values point to oxocarbenium ion-like transition states and further demand that the reaction intermediate have tetrahedral geometry. Evidence for the oxocarbenium ion-like transition states also comes from the tight binding of sugar derivatives with structure and charge distribution similar to that of the transition state (12). Direct evidence for the covalent nature of the glycosyl-enzyme intermediate has been obtained by the trapping of such species using 2-deoxy-2-fluoroglycosides (13). Indeed, such long-lived stable intermediates have now been analyzed at the 3-D level by the X-ray crystallographic analysis of a  $\beta$ -1,4-glycanase and an *S*-glycosidase trapped in this form (14–16). Interestingly, the double-displacement mechanism is not believed to apply to the “textbook” mechanism for the paradigmatic glycosidase, hen egg-white lysozyme, which apparently instead involves an oxocarbenium ion intermediate stabilized electrostatically by an enzymatic carboxylate (1, 2).

In this paper we provide a multidisciplinary analysis of the mechanism of a retaining cellulase, the Cel5A<sup>1</sup> from *Bacillus agaradhaerens*. Cel5A has been analyzed structurally, by X-ray crystallography, in all its stable states along the reaction coordinate: i.e., the free enzyme at atomic (0.95 Å) resolution; the Michaelis complex with unhydrolyzed substrate bound across the active center; the catalytically competent glycosyl-enzyme intermediate (both a fluorocellobiosyl- and a fluorocellotriosyl-enzyme species); and the product-bound form. The structural results, together with

kinetic analysis of the formation and hydrolysis of the covalent glycosyl-enzyme intermediate, provide an unprecedented picture of the catalytic mechanism of retaining glycoside hydrolases and considerable insight into the use of binding energy in enzymatic catalysis.

## EXPERIMENTAL PROCEDURES

**Kinetics.** DNPC, 2FDNPC, and the 2-fluorocellotrioside were synthesized as described previously (17, 18). Buffer chemicals and other reagents were obtained from Sigma Chemical Co. Kinetic studies were performed at 37 °C, in 50 mM sodium phosphate buffer, pH 7.5, containing 0.1% BSA using DNPC as assay substrate as described previously (19). Inactivation parameters,  $k_i$  and  $K_i$ , were determined using six concentrations of the inactivator from 0 to 4.9 mM. Reactivation parameters were determined on purified (by dialysis) 2-fluorocellobiosyl-enzyme in the presence of five concentrations of cellobiose, essentially as described for related systems (19). Mass spectra were recorded using a PE-Sciex API 300 triple quadrupole mass spectrometer (Sciex, Thornhill, Ontario, Canada) equipped with an Ion-spray ion source.

**Crystallization, Structure Solution, and Refinement.** Crystals of the *B. agaradhaerens* Cel5A in space group  $P2_12_12_1$ , with cell dimensions  $a = 54.7$  Å,  $b = 69.6$  Å, and  $c = 77.0$  Å, were grown as previously described for the native structure determination (20). The Michaelis complex of unhydrolyzed substrate was obtained by soaking the crystals overnight in a stabilizing solution with the addition of 5 mM 2,4-dinitrophenyl 2-deoxy-2-fluoro- $\beta$ -D-cellobioside at pH 5.5. Trapped intermediate complexes were obtained by reacting the crystals at pH 7 for 3 h in the presence of 1 mM 2,4-dinitrophenyl 2-deoxy-2-fluoro- $\beta$ -D-cellobioside (for the cellobiosyl covalent intermediate) or 1 mM 2,4-dinitrophenyl 2-deoxy-2-fluoro- $\beta$ -D-cellotrioside (for the cellotriosyl intermediate) followed by crystallization at pH 5.5 as before. The product complex was obtained by soaking in 10 mM  $\beta$ -D-cellotriose for 18 h. Data for structures 3A3H, 4A3H, 5A3H, and 6A3H were collected using a Cu K $\alpha$  rotating anode source with a MARresearch image-plate detector using long-focusing mirror optics. Data for 7A3H were collected at the Daresbury Synchrotron Radiation Source, beamline PX 9.6, using a MARresearch image plate system. All crystallographic computing used the CCP4 suite unless stated otherwise (21). All structures, except 7A3H, were refined with the REFMAC (22) program; 7A3H was refined using both SHELXL97 (23) and REFMAC. The same cross-validation subset of reflections was maintained for refinement of all structures. Coordinates have been deposited with the Brookhaven Protein Data Bank (24). Details of the data and model quality are given in Table 1.

## RESULTS AND DISCUSSION

Cel5A is a member of family 5 of the glycoside hydrolases whose native structure and cellobiose complex were recently determined by X-ray crystallography (20). Glycoside hydrolase family 5 belongs to a “clan” of related structures whose catalytic machinery and stereochemistry of hydrolysis are conserved (3, 4). As such, it displays similarity to a diverse array of enzymes including the *E. coli*  $\beta$ -galactosidase (25) and a number of medically important enzymes such as

<sup>1</sup> Abbreviations: Cel5A, family 5 endoglucanase; DNPC, 2,4-dinitrophenyl  $\beta$ -D-cellobioside.

Table 1: Summary of the Data Collection and Model Statistics for the *B. agaradhaerens* Cel5A

	native (0.95 Å)	Michaelis complex	intermediate 1	intermediate 2	product
ligand	none	DNP2Fcell	2-fluorocellobiosyl-enzyme	2-fluorocellotriosyl-enzyme	cellotriose
resolution (Å) (outer bin)	20–0.95 (0.97–0.95)	15–1.65 (1.72–1.65)	15–1.82 (1.88–1.82)	15–1.68 (1.74–1.68)	15–1.64 (1.7–1.64)
$R_{\text{merge}}$	0.043 (0.31)	0.046 (0.17)	0.061 (0.260)	0.057 (0.31)	0.046 (0.184)
completeness	99.6 (83.8)	99.9 (99.8)	99.7 (99.2)	99.5 (98.3)	99.5 (97.1)
multiplicity	4.2 (4.0)	4.2 (4.2)	4.3 (4.4)	4.2 (4.3)	4.2 (4.2)
$I/\sigma I$	31.8 (3.6)	20.0 (7.7)	16.5 (4.6)	23.9 (4.6)	19.2 (7.6)
$R_{\text{cryst}}$ ( $R_{\text{free}}$ (49))	0.11 (0.12)	0.14 (0.17)	0.14 (0.186)	0.15 (0.18)	14.8 (17.6)
rms bonds (Å)	0.007	0.010	0.010	0.007	0.010
PDB (24) code	7A3H	4A3H	5A3H	6A3H	3A3H

the  $\alpha$ -L-iduronidase involved in Hurler's syndrome. These enzymes all have a regular  $(\beta/\alpha)_8$  "TIM"-barrel fold in which the catalytic acid/base and nucleophile are located on strands  $\beta$ -4 and  $\beta$ -7 of the barrel fold (26, 27). In the case of the *B. agaradhaerens* Cel5A the catalytic acid/base and nucleophile are residues 139 and 228, respectively.

Native diffraction data have been measured to 0.95 Å resolution utilizing synchrotron radiation (Table 1). Atomic resolution data allow us to dissect out atomic features with high precision. Refinement with SHELXL97 (23) allows the protonation states of the carboxylates to be assigned on the basis of the respective C–O bond lengths (28). Such refinement of the catalytic residues Glu 139 and Glu 228 reveals that both nucleophile and acid/base may be protonated in the pH 5.5 native enzyme structure. Additionally of interest is Arg 62, conserved in all family 5-members (29), which forms a 2.9 Å hydrogen bond to the OE1 atom of the catalytic nucleophile Glu 228. Atomic resolution analysis reveals that the guanidino group shows a significant deviation from the expected planarity with the CZ, NH1, NH2 plane rotated approximately 17° out of the CD, NE, CZ plane. A steric barrier to rotation of the NH1 and NH2 atoms around the NE–CZ bond is imposed by stacking of the guanidino group alongside the carboxylate of Asp 99. This geometric perturbation presumably assists in providing an ideal geometric and electrostatic environment for the nucleophile, in particular via the charge-dipole interaction between Glu 228 and Arg 62.

**Enzyme–Substrate Complex.** To observe both the enzyme–substrate complex and the glycosyl-enzyme intermediate, it was necessary to develop methods to slow the chemical steps in the mechanism. Two independent approaches were employed, in concert. The first involved use of enzyme crystals formed at low pH (5.5) where the enzyme is largely inactive, a similar approach having successfully been developed on an unrelated system for the analysis of haloalkane dehalogenase (30). In common with other retaining glycosidases, protonation of the catalytic nucleophile of Cel5A yields an inactive enzyme form (31–33), and indeed such protonation is directly confirmed in this structure by analysis of the bond lengths for the nucleophilic carboxylate group in the 0.95 Å native enzyme structure. Thus, substrates soaked into this crystal form should be converted only very slowly. A second approach involves the use of a substrate in which the sugar 2-hydroxyl has been replaced by an electronegative fluorine substituent. Such substitution both removes hydrogen-bonding interactions which are important in transition state stabilization and also inductively destabilizes the positively charged oxocarbenium ion-like transition state (13, 34). The consequence of such transition state destabilization is extremely slow turnover of this substrate.

Soaking of crystals at pH 5.5 with 2,4-dinitrophenyl 2-deoxy-2-fluoro- $\beta$ -cellobioside (DNP2Fcell) generated the Michaelis complex in which the substrate binds in the –2, –1, and +1 subsites (nomenclature described in ref 35) of the enzyme with the dinitrophenyl moiety occupying the leaving group (+1) subsite with an intact glycosidic bond spanning the active site. The dinitrophenyl group, although not the natural aglycon, binds via hydrophobic stacking interactions with Trp 178 in the +1 subsite of the enzyme, in a manner likely analogous to that used by glycoside hydrolases to bind their more natural substrates (36). The critical feature of this Michaelis complex is the substantial distortion of the –1 subsite sugar away from the preferred  $^4C_1$  conformation into a  $^1S_3$  skew-boat. This results in a quasi-axial orientation for the glycosidic bond being cleaved and has the dramatic effect of placing the leaving group (+1) sugar up to 8 Å away from the position it would otherwise occupy (Figure 2a).

The role for substrate distortion in enzymatic glycoside hydrolysis was first proposed in the late 1960s by Phillips on the basis of the analysis of oligosaccharide complexes of HEWL (2) and confirmed by analysis of a HEWL tetrasaccharide lactone derivative (37). Similar work on product and pseudoproduct complexes of HEWL (38, 39) and bacteriophage T4 lysozyme (40) revealed distorted sugars, but in all of these studies there was no covalent link to the leaving group. The Cel5A structure is thus one of very few to be determined for a  $\beta$ -retaining glycosidase in which an intact substrate spans the active site and the only one for which all complexes have been structurally defined. Two other recent structures, a chitobiase with its uncleaved natural substrate chitobiose (41) and an endoglucanase I (EG I) with a nonhydrolyzable thiooligosaccharide substrate analogue, have likewise revealed similar conformations for the –1 subsite sugar (42, 43). The implications of this distortion for enzymatic glycoside hydrolysis are discussed below.

**Trapping of the Covalent Glycosyl-Enzyme Intermediate.** The next stable species along the reaction coordinate is the glycosyl-enzyme intermediate. This structure was accessed by use of the same DNP2Fcell but in this case reacting the enzyme in solution with this substrate at pH 7, under which conditions the nucleophile is deprotonated and the enzyme is active. The presence of a good leaving group (2,4-dinitrophenolate) in the substrate largely mitigates the rate-retarding effect of the fluorine substituent on the first step, rendering the intermediate kinetically accessible. However, once formed, turnover of this intermediate is very slow. The time-dependent inactivation of the enzyme via formation of the 2-deoxy-2-fluorocellobiosyl-enzyme intermediate follows pseudo-first-order kinetics, allowing determination of kinetic parameters for the formation of the intermediate of  $k_f = 0.063$

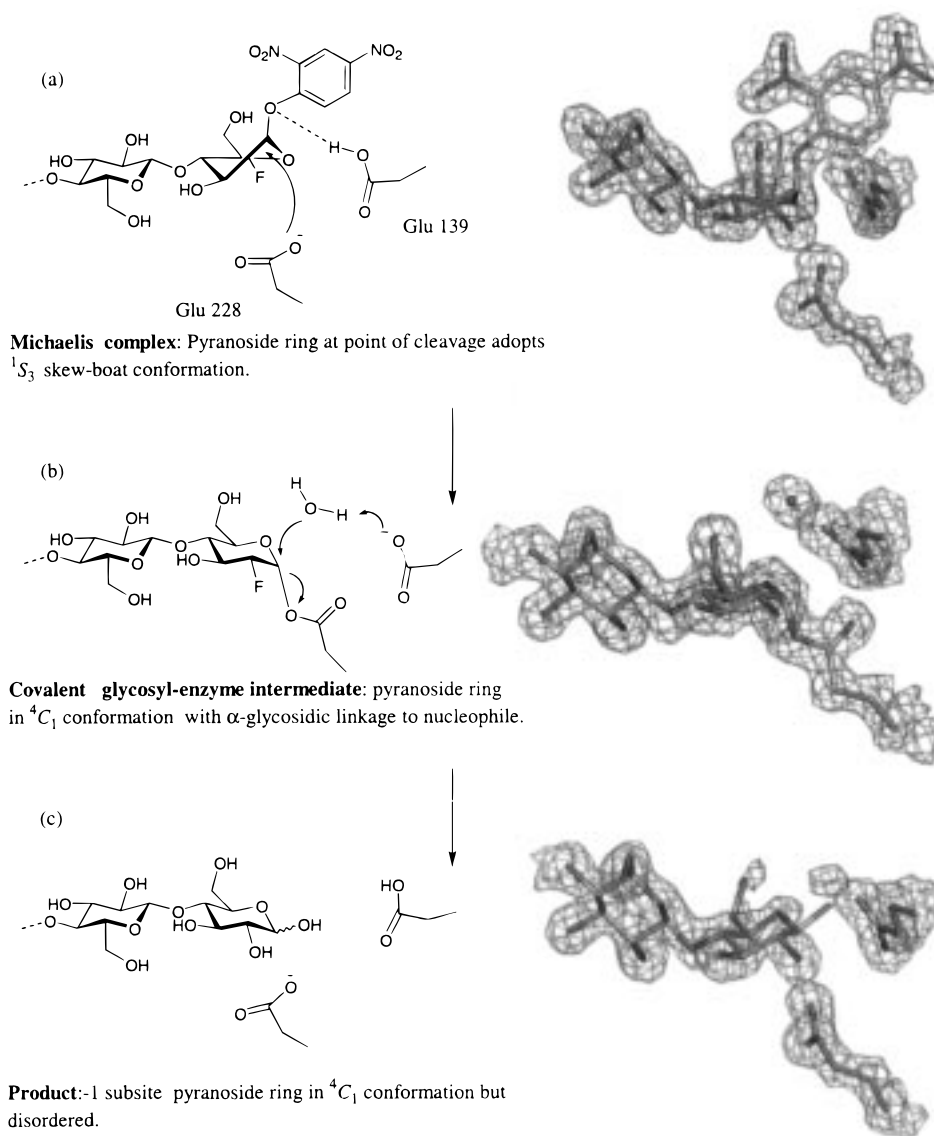


FIGURE 2: Snapshots along a reaction coordinate: (a) Michaelis complex of intact substrate, (b) trapped covalent glycosyl-enzyme intermediate, and (c) product. Electron density at the -3 subsite has been omitted for clarity. The electron density maps shown are maximum-likelihood-weighted  $2F_o - F_c$  syntheses, contoured at approximately  $0.44 \text{ e}/\text{\AA}^3$ .

$\pm 0.002 \text{ min}^{-1}$  and  $K_d = 26.7 \pm 2.1 \text{ }\mu\text{M}$  (Figure 3). The inclusion of a competitive inhibitor, D-cellobiose (101 mM), reduces the observed rate constant for formation of the intermediate, in the presence of  $49 \text{ }\mu\text{M}$  DNP2Fcell, from  $0.0390 \pm 0.0008$  to  $0.010 \pm 0.0006 \text{ min}^{-1}$ , indicating that reaction is occurring at the active site and therefore, by analogy with results from *Agrobacterium*  $\beta$ -glucosidase, that the normal intermediate in catalysis is being trapped (44, 45).

The catalytic competence of the 2-deoxy-2-fluorocellobiosyl-enzyme intermediate was demonstrated by measuring the rate of regeneration of the free enzyme due to turnover, yielding a reactivation rate constant of  $k_{\text{hy}} = 0.00013 \pm 0.00002 \text{ min}^{-1}$ , corresponding to a  $t_{1/2}$  of 88.8 h. As would be expected for a competent glycosyl-enzyme intermediate which can undergo transglycosylation, the addition of D-cellobiose to the 2-deoxy-2-fluorocellobiosyl-enzyme increased the rate of reactivation, the rate observed being dependent on the D-cellobiose concentration in a saturable manner. Kinetic parameters for the reactivation process of  $k_{\text{react}} = 0.0330 \pm 0.0015 \text{ min}^{-1}$  and  $K_{\text{react}} = 248 \pm 17 \text{ mM}$ ,

corresponding to a half-life, at saturating D-cellobiose, of 21 min were determined (Figure 4). This formation of a stoichiometric (1:1) glycosyl-enzyme complex was confirmed by ion spray mass spectrometry.

Crystallographic analyses of both the trapped 2-deoxy-2-fluorocellobiosyl-enzyme intermediate and the 2-deoxy-2-fluorocellobiosyl-enzyme intermediate were achieved through incubation of the enzyme in solution with a 1 mM quantity of the relevant substrate for 3 h at pH 7.5, followed by dropping the pH to 5.5 prior to crystallization and structure determination. One beneficial consequence of lowering the pH for the crystallization is that the deglycosylation (reactivation) rate constant is further reduced since protonation of the catalytic acid/base prevents it functioning as a Brønsted base in the hydrolysis of the trapped intermediate. The unbiased electron density at  $1.65 \text{ }\text{\AA}$  resolution shows unambiguously that the enzyme has been trapped as its covalent glycosyl-enzyme intermediate (Figure 2b). A water molecule is also seen poised above the pyranoside ring, hydrogen-bonding to the prospective catalytic acid/base Glu 139, in perfect position for nucleophilic attack on the



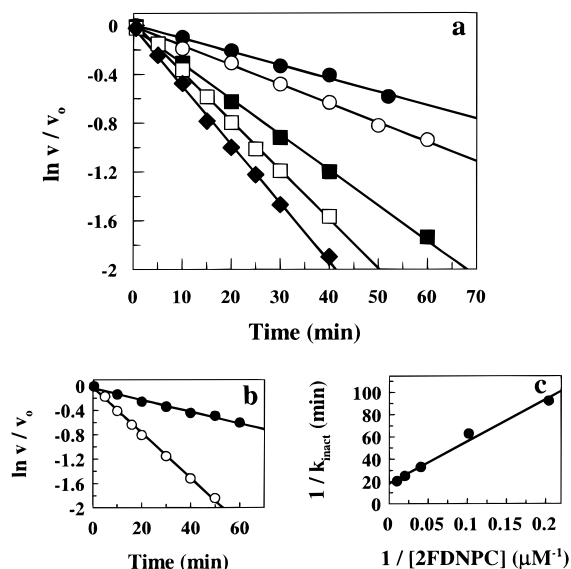


FIGURE 3: Inactivation of *B. agaradhaerens* Cel5A by 2FDNPC. (a) Semilogarithmic plot of residual activity vs time at the indicated 2FDNPC concentrations: (●) 4.9  $\mu\text{M}$ , (○) 9.8  $\mu\text{M}$ , (■) 24.5  $\mu\text{M}$ , (□) 49.0  $\mu\text{M}$ , and (◆) 98.0  $\mu\text{M}$ . (b) Inactivation with 49.0  $\mu\text{M}$  2FDNPC in the (○) absence and (●) presence of 101 mM D-cellobiose. (c) Replot of the first-order rate constants from (a).

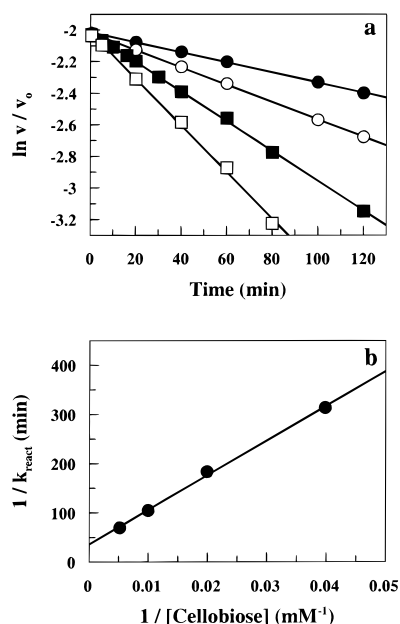


FIGURE 4: Reactivation of 2-deoxy-2-fluorocellobiosyl Cel 5A by D-cellobiose. (a) Semilogarithmic plot of activity vs time for (●) 25.3 mM, (○) 50.5 mM, (■) 101 mM, and (□) 192 mM BTC. (b) Double-reciprocal replot of first-order rate constants from (a) vs D-cellobiose concentration.

glycosyl-enzyme. This water occupies essentially the same position taken by the glycosidic oxygen in the Michaelis complex, as expected for a reaction involving a simple substitution at the sugar anomeric center. The  $-1$  subsite sugar is in an undistorted  ${}^4C_1$  chair conformation with an  $\alpha$ -linkage to the enzymatic nucleophile Glu 228 similar to that observed in the myrosinase glycosyl-enzyme intermediate (15) but somewhat different from the slightly distorted 2-fluorocellobiosyl-enzyme reported for the *Cellulomonas fimi* Cex (14). Interestingly, whereas in the structures of 2-fluorocellobiosyl- and 2-fluoroxyllobiosyl-Cex, as well as the myrosinase, the carbonyl oxygen of the catalytic nucleophile

is held in close proximity to the C-2 fluorine, this is not the case for the Cel5A structure, the carboxyl group having rotated outward and a water having occupied its position. One consequence of this is the loss of the interaction with Arg 62, which was probably crucial for correct orientation of the nucleophile for the glycosylation step. Apparently the active site of the Cel5A enzyme is sufficiently flexible to allow this movement, thereby minimizing the destabilizing interaction between the fluorine and the oxygen. The structures of the other enzymes appear to be too rigid to allow this. In Cel5A the active site clearly tolerates side-chain movement "in-crystal". This flexibility manifests itself in dual conformations for both the O-6 hydroxyl of the  $-1$  subsite sugar and the side chain of Tyr 202. Tyr 202, disordered in the 0.9 Å native structure, is found in two discrete conformations in the cellobiosyl and cellotriosyl intermediates. In one conformation, the hydroxyl group interacts with the new conformation of Glu 228, whereas the second orientation of Tyr 202 interacts with one of the two conformations of the  $-1$  subsite O-6 hydroxyl. Strangely, the predominant conformation for Tyr 202 is different in the cellotriosyl and cellobiosyl complexes, the former interacting more closely with the O-6 and the latter with Glu 228. Other than this, the interactions of the cellobiosyl and cellotriosyl species are conserved. The  $-3$  subsite interactions of the cellotriosyl species are essentially identical to that seen in the cellotriose product complex.

**The Product Complex.** The three-dimensional structure of the product complex was analyzed by soaking the native crystals in an excess of the free product; in this case  $\beta$ -D cellotriose. The reaction product is seen to bind in the  $-3$ ,  $-2$  and  $-1$  subsites, as expected. While the density for the  $-3$  and  $-2$ , subsite sugars is extremely well-defined, the  $-1$  subsite sugar exhibits a great deal of disorder, with little defined density for C-6, O-6, C-2, O-2, C1, and O1 (Figure 2c). This presumably results from the absence of specific stabilizing interactions at that end of the molecule or from unfavorable, destabilizing interactions. At low contour levels there is evidence for both the  $\alpha$ - and  $\beta$ -anomers, presumably as a result of mutarotation. Although this complex displays disorder, there is no evidence for any static distortion of the reducing end ring away from a chair conformation as was observed for the Michaelis complex (Figure 2a). Together, these observations suggest that the distortion seen in the substrate complex may be driven by the additional interactions of the aglycon in the  $+1$  subsite which are clearly not accessible to the product.

**Implications for Enzymatic Glycoside Hydrolysis and Inhibitor Design.** Recently, three separate structure determinations of glycosyl hydrolases with uncleaved substrates spanning the active site have revealed a remarkable distortion of the pyranoside ring at the site of enzymatic cleavage, in which the ring is twisted away from its normal  ${}^4C_1$  chair conformation toward a skew-boat. Sugar binding sites of these structurally unrelated enzymes all undergo a marked "kink" at the active site, such that a regular polymer of  $\beta$ -D-sugars in  ${}^4C_1$  conformation would be unable to bind across the point of cleavage. In the two highest resolution and most well-defined of these analyses the pyranoside ring can be unambiguously described as adopting a  ${}^1S_3$  skew-boat conformation. These unhydrolyzed saccharides have been trapped on-enzyme by three separate means: nonhydrolyz-

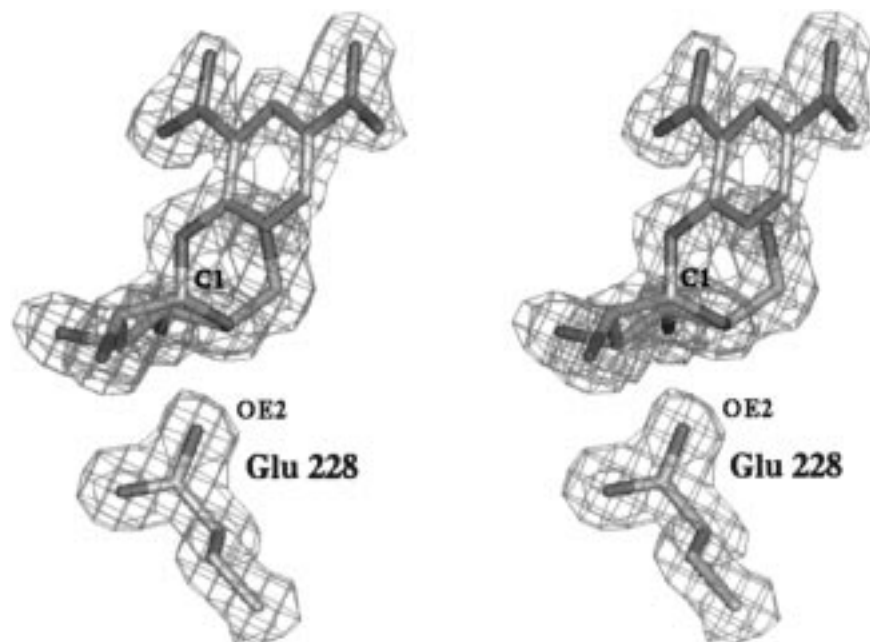


FIGURE 5: Stereographic “end-on” section through the electron density for the unhydrolyzed substrate complex of Cel5A. The enzymatic nucleophile, Glu 228, is shown, as are the  $-1$  subsite pyranoside ring atoms and the dinitrophenyl leaving group. Substrate distortion to a skew-boat conformation permits nucleophilic attack “in-line” with leaving group departure.

able sulfur-containing substrate analogues (42, 43), short crystallographic soaking times to trap an otherwise thermodynamically unfavored species (41), and, in this case, by the utilization of an acidic pH at which the enzyme is inactive, coupled with a poorly hydrolyzable fluorosugar substrate. A major consequence of this pyranoside ring contortion is the displacement of the adjacent ( $+1$  subsite) moiety by over 8 Å compared to the position that would be occupied by the aglycon of a sugar with a regular  $\beta$ -linkage between two  ${}^4C_1$  ring sugars. Such distortion must be primarily driven by the extra interactions that develop within the  $+1$  (leaving group) subsite since species which do not bind in that site (bound products and the covalent intermediate) are undistorted. This observation is of considerable significance for those embarked on inhibitor and drug design programs for glycosidases and other glycosyl transferases. This substrate distortion confers many catalytic benefits to the enzyme, as follows. Direct attack on the sugar anomeric center by the nucleophile, concomitant with leaving group departure, would require an in-line approach. The problem facing the enzyme is that such attack is sterically hindered, both by the hydrogen atom bound to C-1 and by the H-3 and H-5 protons. This concept is well documented elsewhere since Bentley and Schleyer, among others, demonstrated a lack of  $S_N2$  nucleophilic attack on conformationally restricted 2-adamantyl substrates due to analogous steric hindrance (46). In order for the enzyme to make a nucleophilic substitution at C1, the sugar must first be distorted away from its ground-state  ${}^4C_1$  chair conformation toward a boat or skew-boat form in which the glycosidic bond and leaving group become axial (Figure 5). This is exactly what is observed in the EG I, chitobiase, and Cel5A complex structures. Distortion in this direction also moves the substrate closer to the conformation of the oxocarbenium ion transition state, in addition to presenting the glycosidic oxygen in an appropriate position for protonation by the enzymatic Brønsted acid. Such was not the case for the

bound sugar in its ground-state  ${}^4C_1$  chair conformation with the glycosidic bond equatorial to the ring plane. Additionally, the pseudoaxial glycosidic bond orientation is consistent with the dictates of stereoelectronic theory, which posits that hydrolysis rates are enhanced by the overlap of the ring oxygen lone pair electrons with the antibonding orbitals of the glycosidic bond, thus requiring an antiperiplanar arrangement of the lone pair orbitals and the scissile bond (47, 48).

It is 30 years since the pioneering work of Sir David Phillips and co-workers on complexes of HEWL led to proposals concerning the importance of substrate distortion during glycoside hydrolysis. Analysis of the structure of HEWL oligosaccharide complexes together with an appreciation of the concepts of transition-state theory as applied to enzymatic systems revealed the probable role of substrate distortion in glycoside hydrolysis. The structure determinations described here of another class of glycosidase with uncleaved oligosaccharides both spanning the active site and trapped in their covalent-enzyme intermediate state reveal the full nature of the role of binding energy in catalysis and the magnitude and importance of substrate distortion and point toward their wide applicability and importance.

## REFERENCES

1. Blake, C. C. F., Koenig, D. F., Mair, G. A., North, A. C. T., Phillips, D. C., and Sarma, V. R. (1965) *Nature* 206, 757–763.
2. Blake, C. C. F., Johnson, L. N., Mair, G. A., North, A. C. T., Phillips, D. C., and Sarma, V. R. (1967) *Proc. R. Soc. London, Ser. B* 167, 378–388.
3. Henrissat, B., and Bairoch, A. (1996) *Biochem. J* 316, 695–696.
4. Henrissat, B., and Davies, G. J. (1997) *Curr. Opin. Struct. Biol.* 7, 637–644.
5. Davies, G., and Henrissat, B. (1995) *Structure* 3, 853–859.
6. Jacob, G. S. (1995) *Curr. Opin. Struct. Biol.* 5, 605–611.
7. von Itzstein, M., and Colman, P. (1996) *Curr. Opin. Struct. Biol.* 6, 703–709.

8. Gebler, J., Gilkes, N. R., Claeysens, M., Wilson, D. N., Béguin, P., Wakarchuk, W. W., Kilburn, D. G., Miller, R. C., Jr., Warren, R. A. J., and Withers, S. G. (1992) *J. Biol. Chem.* **267**, 12559–12561.
9. Koshland, D. E. (1953) *Biol. Rev.* **28**, 416–436.
10. McCarter, J. D., and Withers, S. G. (1994) *Curr. Opin. Struct. Biol.* **4**, 885–892.
11. Davies, G., Sinnott, M. L., and Withers, S. G. (1997) in *Comprehensive Biological Catalysis* (Sinnott, M. L., Ed.) pp 119–209, Academic Press, London.
12. Legler, G. (1990) *Adv. Carbohydr. Chem. Biochem.* **48**, 319–385.
13. Withers, S. G., Street, I. P., Bird, P., and Dolphin, D. H. (1987) *J. Am. Chem. Soc.* **109**, 7530–7531.
14. White, A., Tull, D., Johns, K., Withers, S. G., and Rose, D. R. (1996) *Nat. Struct. Biol.* **3**, 149–154.
15. Burmeister, W. P., Cottaz, S., Driguez, H., Palmieri, S., and Henrissat, B. (1997) *Structure* **5**, 663–675.
16. Notenboom, V., Birsan, C., Warren, R. A. J., Withers, S. G., and Rose, D. R. (1998) *Biochemistry* **37**, 4751–4758.
17. McCarter, J. D., Adam, M. J., Braun, C., Namchuk, M. N., Tull, D., and Withers, S. G. (1993) *Carbohydr. Res.* **249**, 77–90.
18. Mackenzie, L. F., Wang, Q., Warren, R. A. J., and Withers, S. G. (1998) *J. Am. Chem. Soc.* **120**, 5583–5584.
19. Wang, Q., Tull, D., Meinke, A., Gilkes, N. R., Warren, R. A. J., Aebersold, R., and Withers, S. G. (1993) *J. Biol. Chem.* **268**, 14096–14102.
20. Davies, G. J., Dauter, M., Brzozowski, A. M., Bjornvad, M. E., Anderson, K. V., and Schülein, M. (1998) *Biochemistry* **37**, 1926–1932.
21. Collaborative Computational Project Number 4 (1994) *Acta Crystallogr. D50*, 760–763.
22. Murshudov, G. N., Vagin, A. A., and Dodson, E. J. (1997) *Acta Crystallogr. D53*, 240–255.
23. Sheldrick, G. M., and Schneider, T. R. (1997) *Methods Enzymol.* **277**, 319–343.
24. Bernstein, F. C., Koetzle, T. F., Williams, G. J. B., Meyer, E. T., Jr., Brice, M. D., Rodgers, J. R., Kennard, O., Shimanouchi, T., and Tasumi, M. (1977) *J. Mol. Biol.* **112**, 535–542.
25. Jacobson, R. H., Zhang, X.-J., DuBose, R. F., and Matthews, B. W. (1994) *Nature* **369**, 761–766.
26. Henrissat, B., Callebaut, I., Fabrega, S., Lehn, P., Mornon, J.-P., and Davies, G. (1995) *Proc. Natl. Acad. Sci. U.S.A.* **92**, 7090–7094.
27. Jenkins, J., Leggio, L. L., Harris, G., and Pickersgill, R. (1995) *FEBS Lett.* **362**, 281–285.
28. Dauter, Z., Lamzin, V. S., and Wilson, K. S. (1997) *Curr. Opin. Struct. Biol.* **7**, 681–688.
29. Sakon, J., Adney, W. S., Himmel, M. E., Thomas, S. R., and Karplus, P. A. (1996) *Biochemistry* **35**, 10648–10660.
30. Verschuren, K. H. G., Seljée, F., Rozeboom, H. I., Kalk, K. H., and Dijkstra, B. W. (1993) *Nature* **363**, 693–698.
31. Tull, D., and Withers, S. G. (1994) *Biochemistry* **33**, 6363–6370.
32. Kempton, J. B., and Withers, S. G. (1992) *Biochemistry* **31**, 9961–9969.
33. McIntosh, L. P., Hand, G., Johnson, P. E., Joshi, M. D., Körner, M., Plesniak, L. A., Ziser, L., Wakarchuk, W. W., and Withers, S. G. (1996) *Biochemistry* **35**, 9958–9966.
34. Withers, S. G., and Aebersold, R. (1995) *Protein Sci.* **4**, 361–372.
35. Davies, G. J., Wilson, K. S., and Henrissat, B. (1997) *Biochem. J.* **321**, 557–559.
36. Vyas, N. K. (1991) *Curr. Opin. Struct. Biol.* **1**, 732–740.
37. Ford, L. O., Johnson, L. N., Machin, P. A., Phillips, D. C., and Tjian, T. (1974) *J. Mol. Biol.* **88**, 349–371.
38. Strynadka, N. C. J., and James, M. N. G. (1991) *J. Mol. Biol.* **220**, 401–424.
39. Hadfield, A. T., Harvey, D. J., Archer, D. B., MacKenzie, D. A., Jeenes, D. J., Radford, S. E., Lowe, G., Dobson, C. M., and Johnson, L. N. (1994) *J. Mol. Biol.* **243**, 856–872.
40. Kuroki, R., Weaver, L. H., and Matthews, B. W. (1993) *Science* **262**, 2030–2033.
41. Tews, I., Perrakis, A., Oppenheim, A., Dauter, Z., Wilson, K. S., and Vorgias, C. E. (1996) *Nat. Struct. Biol.* **3**, 638–648.
42. Sulzenbacher, G., Driguez, H., Henrissat, B., Schülein, M., and Davies, G. J. (1996) *Biochemistry* **35**, 15280–15287.
43. Sulzenbacher, G., Schülein, M., and Davies, G. J. (1997) *Biochemistry* **36**, 5902–5911.
44. Withers, S. G., and Street, I. P. (1988) *J. Am. Chem. Soc.* **110**, 8551–8553.
45. Withers, S. G., Warren, R. A. J., Street, I. P., Rupitz, K., Kempton, J. B., and Aebersold, R. (1990) *J. Am. Chem. Soc.* **112**, 5887–5889.
46. Bentley, T. W., and Schleyer, P. v. R. (1977) *Adv. Phys. Org. Chem.* **14**, 1–67.
47. Deslongchamps, P. (1983) *Stereoelectronic Effects in Organic Chemistry*, Pergamon Press, Oxford.
48. Kirby, A. J. (1984) *Acc. Chem. Res.* **17**, 305–311.
49. Brünger, A. T. (1992) *Nature* **355**, 472–475.

BI981315I